LNF-88/63

A. Di Cicco, A. Bianconi, M. Benfatto, A. Marcelli, C.R. Natoli, P. Pianetta, J. Woicik

ORIENTATIONAL DISORDER IN AMORPHOUS SILICON PROBED BY XANES (X-RAY ABSORPTION NEAR EDGE STRUCTURE)

Estratto da: Phys. Scripta 38, 408 (1988)

Physica Scripta. Vol. 38, 408–411, 1988.

Orientational Disorder in Amorphous Silicon Probed by XANES (X-ray Absorption near Edge Structure)*

A. Di Cicco and A. Bianconi

Dipartimento di Fisica, Università di Roma "La Sapienza", 00185 Roma, Italy

M. Benfatto, A. Marcelli and C. R. Natoli

Istituto Nazionale di Fisica Nucleare, Laboratori Nazionali di Frascati, 00044 Frascati, Italy

and

P. Pianetta and J. Woicik

Stanford Synchrotron Radiation Laboratory, Stanford University, California 94305, U.S.A.

Received July 7, 1987; accepted March 25, 1988

Abstract

The difference between the *K*-edges XANES (X-ray Absorption Near Edge Structure) spectra of crystal and amorphous silicon is discussed. We show that the multiple scattering signal gives a large contribution to the total absorption in crystalline silicon in an energy range of about 70 eV. The double scattering term probing the triplet distribution function gives the major contribution to the XANES. We show that the difference between the crystalline and amorphous absorption spectra is due mainly to the crystalline multiple scattering signal which is quenched in the amorphous spectrum. The suppression of the signal due to the triplet distribution function in the amorphous silicon is assigned to the large orientational disorder.

1. Introduction

In amorphous materials two different kind of disorder can be identified: first, the disorder in interatomic distances which is probed by the pair distribution function; second, the disorder in bond angles which is probed by the higher order distribution functions. X-ray absorption spectroscopy can provide information on both types of order in condensed systems by switching the focus of data analysis from the EXAFS part (extended X-ray absorption fine structure) [1, 2] to the XANES part (X-ray absorption near edge fine structure) [3–8] of the absorption spectrum. In fact, EXAFS gives information about interatomic distances and coordination numbers and XANES provides information on bond angles [5] and the triplet distribution function can be extracted in some cases [7].

For crystals it has been demonstrated that the description of the optical transitions in terms of the classical Fermi golden rule in the *k*-space is equivalent to the multiple scattering description in the real space in a small cluster around the photoabsorbing atom [9, 10]. In this way there is an exact correspondence between band theory description of the electron states and multiple scattering formalism. The size of the cluster considered in a multiple scattering calculation is determined by the inelastic mean free path of the photoelectron and the core hole lifetime [11]. The advantage of the multiple scattering (MS) approach is that it can be extended to materials where there is not long range order and therefore information on local structure can be determined.

In a recent paper [11] we showed how the multiple scattering signal can be extracted from an experimental spectrum and that multiple scattering effects can explain the main structures of the absorption spectra of crystal silicon in the first 70 eV beyond the *K*-threshold. In some other recent papers [12, 13] the energy range of multiple scattering has been subject of discussion. Infact the case of copper *K*-edge [13] exhibits weak multiple scattering effects. It was suggested that in the case of open structures, with no atoms in collinear configuration, multiple scattering is negligible. We have focused our attention on the silicon crystal where in the local structure (in a cluster of 99 atoms) there are no atoms in collinear configuration and where the EXAFS spectrum can be calculated *ab initio* [11]. This work shows that the difference between the XANES spectra of crystalline and amorphous silicon is mainly due to the suppression of the peaks due to the triplet distribution function. Orientational disorder in bond angles of amorphous silicon can explain the suppression of this relevant multiple scattering signal.

2. Experimental

The *K*-edge absorption spectra of crystalline and amorphous silicon have been determined by measuring the intensity of the *KLL* Auger emission as a function of the photon energy. The measurements were performed using the Jumbo monochromator at the Stanford Synchrotron Radiation Laboratory.

The signal was normalized to the incident flux, I_0, and the intensity of the Auger emission was measured with a double pass cylindrical mirror analyzer which was set at the silicon *KLL* Auger peak at 1610 eV. The data were collected in constant final state mode as the photon energy was swept across the absorption edge.

The amorphous silicon sample was prepared in an ultra-high vacuum chamber ($p < 10^{-10}$ torr) by depositing > 200 Å of silicon by electron beam evaporation onto a germanium substrate which was held at room temperature throughout the evaporation.

* Paper presented at the 7th General Conference of the CMD-EPS, Pisa, 7–10 April 1987.

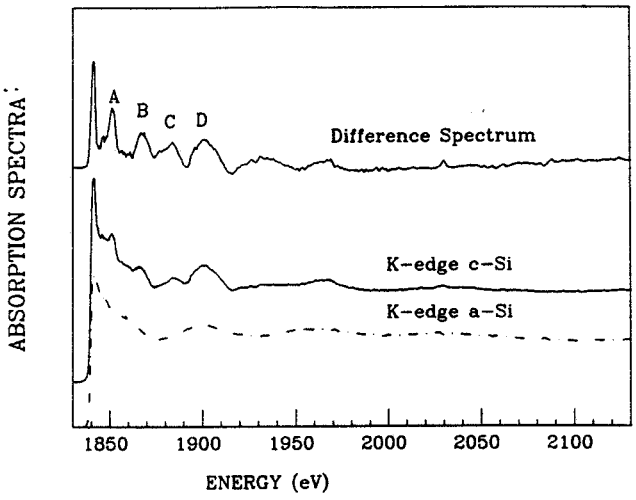

Fig. 1. X-ray absorption spectra of crystalline and amorphous silicon determined by measuring the intensity of the KLL Auger emission as a function of the photon energy. The upper curve shows the difference spectrum $(\alpha_{cr} - \alpha_{am}) \times 2$ between the two absorption spectra.

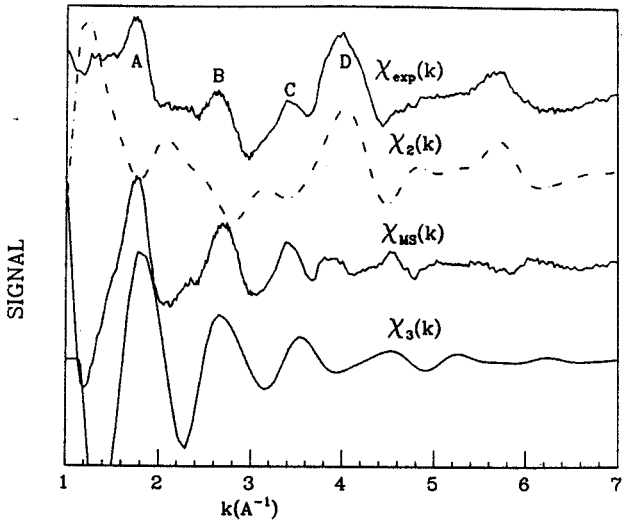

Fig. 2. Experimental $\chi_{exp}(k)$ (upper curve) compared with: the calculated $\chi_2(k)$ spectrum (dot-dashed curve); the difference spectrum $\chi_{MS}(k) = \chi_{exp}(k) - \chi_2(k)$ (central solid curve); a theoretical calculation of the $\chi_3(k)$ contribution performed taking into account the most important pathways of double scattering (lower curve). It is a remarkable result to verify that the A, B, C peaks arise mainly from the multiple scattering contribution.

3. Results and discussion

In Fig. 1 the X-ray absorption spectra of crystal and amorphous silicon are reported.

We first consider the case of the *K*-edge of crystal silicon. A good fitting of the EXAFS oscillations from 50 to 450 eV above the absorption threshold ($E_T \approx 1839$ eV) has been obtained using the exact spherical wave EXAFS analysis [11, 14] and the spherical wave approximation (SWA) [10, 11, 15]. The best agreement with the experimental spectrum [16] $\chi_{exp}(k) = [\alpha(k)\ 7\ \alpha_0(k) - \alpha_0(k)]/\alpha(k)$ has been obtained including seven shells around the absorbing atom. In both calculations we have used the same physical parameters $\lambda_{eff}(E)$ and $\sigma^2(R_i)$. The mean free path damping factor $\exp(-2R_i/\lambda_{eff})$, where R_i is the distance of the i-th shell, has been evaluated starting from photoemission measurements considering also the finite core hole lifetime [11, 17]. The Debye-Waller relative terms $\sigma^2(R_i)$ have been evaluated starting from a calculation of Walker and Keating [18, 19]. The EXAFS calculation shows that the first three shells give the major contribution to the spectrum.

The data analysis of the XANES spectra is based on the recent demonstration that in many cases the absorption coefficient can be expanded in the following form [6–8, 10, 11, 15]:

$$\alpha(k) = \alpha_0(k)\left[1 + \sum_{n=2}^{\infty} \chi_n(k)\right] \qquad (1)$$

Here $\alpha_0(k)$ is the structureless absorption coefficient of a central photoabsorbing atom and $\chi_n(k)$ represents the contribution arising from all MS pathways p_n beginning and ending at the central atom and involving $n - 1$ neighboring atoms. The $\chi_2(k)$ term defined in the eq. 1 is determined by single scattering and it is called the EXAFS signal; generally it is the dominant term above wave vector values $k > 4$ Å^{-1}. The $\chi_3(k)$ term is the double scattering signal arising from all the triangular paths with on a vertex the central atom. The general mathematical expression from $\chi_n(k)$ is given by [10, 15]:

$$\chi_n^l(k) = \sum_{p_n} A_n^l(k, p_n) \sin(kR p_n + \phi_n^l(k, p_n) + 2\delta_l^0) \qquad (2)$$

where the dependence of the amplitude and phase function A_n^l and ϕ_n^l on the particular path has been indicated symbolically by p_n and δ_l^0 is the central atom l-th phase shift. General expressions for calculating the quantities A_n^l and ϕ_n^l in terms of the atomic phase shifts and the geometry of the path p_n are provided by the MS theory.

Due to the general structure of the $\chi_n^l(k)$ quantities, the amplitudes A_n^l's decrease with increasing order n, so that usually $\chi_2^l(k)$ is the dominant term in the whole energy range where the series converges. Hence an analysis of the MS contribution beyond the first term is possible if the $\chi_2^l(k)$ contribution is subtracted from the experimental signal:

$$\chi_{exp}(k) = [\alpha(k) - \alpha_0(k)]/\alpha_0(k) \qquad (3)$$

provided a good estimate for $\alpha_0(k)$ is used.

The key point however is to determine in which energy range the MS series in eq. (1) converges for the actual system under investigation. The theoretical condition for convergence is that the spectral radius of the MS matrix $\varrho(T_a G)$ [8, 10] is less than 1. The energy range where there is no convergence can be very small like in tetrahedral clusters [8] and generally it is reduced by finite core hole lifetime, damping of the photoelectron in the final state, limited experimental resolution and thermal and configurational disorder when present. Hence it is a reasonable ansatz to assume that for silicon the MS series converges right from the edge and that the spectra can be analyzed on the basis of the eq. (1).

The multiple scattering signal is defined as $\chi_{MS}(k) = \Sigma_{n=3}^{\infty}\chi_n(k)$ and it can be obtained experimentally by subtraction of a $\chi_2(k)$ spherical waves calculation from the experimental oscillatory part of an absorption spectrum $\chi_{exp}(k)$; therefore $\chi_{MS}(k) = \chi_{exp}(k) - \chi_2(k)$. Following this subtraction procedure over the full experimental energy range from about 5 eV above the threshold we found [11, 15] a strong signal in the first 70 eV above the absorption *K*-edge of silicon which is not possible to explain within the frame of the single scattering formalism. The result of the subtraction is plotted in Fig. 2 (central solid curve). The resulting $\chi_{exp}(k)$ is also

shown in Fig. 2 and it is compared with an EXAFS calculation which has been performed by using the SWA formalism (dot-dashed curve). Looking at Fig. 2 it is clear that the A, B, C peaks arise mainly from multiple scattering effects.

Since the first higher order term in the MS series is the $\chi_3(k)$ term we have performed a calculation of the contributions arising from the double scattering paths involving two neighbour atoms within the first three shells. The resulting $\chi_3(k)$ curve is shown in Fig. 2 (lower curve). We have taken into account mean free path damping effects. There are 756 paths of double scattering within the first three shells and it is possible to sort them out in 41 groups according to total length and scattering angles relative to the central atom. The groups with low path degeneracy are generally negligible since they give only a weak signal. Moreover we can neglect the contribution due to the groups with a very long total length (the perimeter of the triangle) since the mean free path term suppresses their contribution to the spectrum in the energy range beyond 15 eV above the edge, as we have verified.

The main contribution to the χ_3 signal is due to the 36 double scattering paths with the shortest total length ($R_{tot} = 8.54$ Å). These 36 paths can be divided into two groups differing in the angles between the outgoing and incoming paths directed at the photoabsorbing vertex. The first of these two groups comprises 12 paths contained within the first neighbour shell (3S1-type paths) but its contribution to the absorption spectrum is very weak. The second group comprises 24 paths (3S2-type paths) involving the atoms of the second shell and gives the main contribution to the total χ_3 signal. We have verified that in the XANES region the contribution of one 3S2-type path is 6 times greater than the signal due to one 3S1-type path. This is due to the angular dependence of the scattering amplitude of MS paths.

The calculated χ_3 is close to the experimental oscillation χ_{MS} as shown in Fig. 2. The differences between χ_{MS} and the theoretical χ_3 which become more important at low energy can be assigned to higher orders ($n > 3$) of multiple scattering contribution.

The final result is that in the first 70 eV of the *K*-edge absorption spectrum of crystal silicon the multiple scattering contribution is important and the double scattering signal due to the shortest triangular paths can be recognized in the experimental spectrum.

The comparison of Si *K*-edge spectra of amorphous and crystalline silicon is illuminating for the comprehension of Si spectrum in the amorphous phase. The difference spectrum $\alpha_{cr} - \alpha_{am}$ is reported in Fig. 1 (upper curve).

In the absorption spectra of amorphous silicon we expect a χ_2 contribution due to the first coordination shell similar to that one found in the crystal silicon ones. On the contrary the second shell χ_2 signal can be described through a modified Debye–Waller expression composed of two terms [20]: the thermal disorder term σ_T^2 and the configurational disorder term σ_C^2. The signals due to further shells are almost totally suppressed by structural disorder.

However a reliable evaluation of the contribution to an absorption spectrum due to the other coordination shells in amorphous materials is generally difficult to obtain because: (a) The presence of order at certain distances depends on the growth of the sample. (b) Generally a simple Debye–Waller term cannot describe the distribution of distances in a disordered system because the distribution function $g(R)$ can be asymmetric around the broad peaks due to the coordination shells.

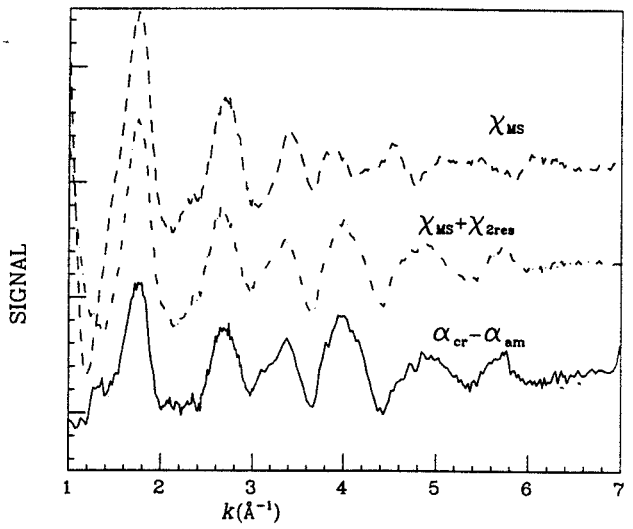

Fig. 3. Modulating part of the difference spectrum $\alpha_{cr}(k) - \alpha_{am}(k)$ (solid curve) in comparison with the crystalline $[\chi_{MS}(k)]_{cr}$ spectrum (χ_{MS}, dashed curve) and the sum of this multiple scattering signal with the single scattering residual $\{[\chi_2(k)_{cr} - [\chi_2(k)]_{am}\}$(dot-dashed curve, $\chi_{MS} + \chi_{2res}$). We observe a perfect agreement of the last curve with the solid one. This fact confirms the presence of a quenching effect of the multiple scattering signal in the amorphous phase.

Therefore in order to obtain a reliable approximation of the contribution of the distant shell we need knowledge of the distribution function, i.e. precise structural information.

In any case a good fit of the amorphous Si *K*-edge spectrum has been obtained over the energy range above about 20 eV beyond threshold by a χ_2 term with only two shells around the photoabsorber [21] (the Debye–Waller term relative to the second shell is considerably greater, $\sigma_{am}^2 \approx 0.08$ Å^2, than the one used for the crystalline silicon: $\sigma_{cr}^2 \approx 0.0073$ Å [11]). Therefore it is reasonable to conclude that the contribution due to the distant shells and multiple scattering effects are almost negligible as long as we look at the energy region above 20 eV beyond the *K*-edge.

The difference between the crystal and the amorphous silicon spectra can be explained, assuming that the atomic absorption α_0 is the same in the two phases, by using the series expansion of the absorption coefficient:

$$\begin{aligned}\sigma_{cr}(k) - \alpha_{am}(k) &= \alpha_0(k)\{1 + [\chi_2(k)]_{cr} + [\chi_{MS}(k)]_{cr}\} \\ &\quad - \alpha_0(k)\{1 + [\chi_2(k)]_{am} + [\chi_{MS}(k)]_{am}\} \\ &= \alpha_0(k)\{[\chi_2(k)]_{cr} - [\chi_2(k)]_{am} \\ &\quad + [\chi_{MS}(k)]_{cr} - [\chi_{MS}(k)]_{am}\}\end{aligned}$$

therefore:

$$[\alpha_{cr}(k) - \alpha_{am}(k)]/\alpha_0(k) = [\chi_{MS}(k)]_{cr} + \{[\chi_2(k)]_{cr} - [\chi_2(k)]_{am}\} - [\chi_{MS}(k)]_{am} \quad (4)$$

In Fig. 3 we have reported the modulating part of $[\alpha_{cr} - \alpha_{am}]/\alpha_0$ (solid curve). In this way we can directly compare this curve with the right hand side (r.h.s) of eq. (4), which is composed of three terms: the MS contribution to the crystalline absorption spectrum, the single scattering residual $\chi_{2res}(k) = [\chi_2(k)]_{cr} - [\chi_2(k)]_{am}$ and the MS contribution to

the amorphous absorption spectrum. The leading term in the XANES energy region is the first and in Fig. 3 we report the $[\chi_{MS}(k)]_{cr}$ (dashed curve) which is close to $[\alpha_{cr} - \alpha_{am}]/\alpha_0$ in the first 45 eV above the edge ($k < 3.5\,\text{Å}^{-1}$). The second term becomes more important in an intermediate energy region ($3\text{–}6\,\text{Å}^{-1}$). In fact, the amorphous spectrum contains $[\chi_2(k)]_{am}$ contributions due to the second shell only in the XANES part of the spectrum because the large Debye–Waller factors quenches this signal rapidly with the increasing energy; therefore in the subtraction we can find these contributions only in an intermediate region of wave vector values. The contribution due to distant shells has been considered in the calculation of the $[\chi_2(k)]_{cr}$ but the signal is weak also in the XANES region in comparison with the MS contribution. In Fig. 3 the sum of the first two terms $\{[\chi_{MS}(k)]_{cr} + \chi_{2res}(k)\}$ of the eq. (4) has been reported (dot-dashed curve). There is a *very good* agreement with the experimental solid curve: the single scattering residual provides the explanation for the presence of the D peak in the $[\alpha_{cr} - \alpha_{am}]/\alpha_0$ curve and the reduction of amplitude observed in the difference spectrum in comparison with the χ_{MS} spectrum is due to the second and further shells contribution in the crystalline spectrum. The final step is the subtraction of the $[\chi_{MS}(k)]_{am}$ in order to test eq. (4) and to obtain the best agreement with the solid curve.

It is well known that the standard deviation in the bond angle distribution of amorphous silicon from tetrahedral coordination is about 10^0 [35, 36]. This disorder in bond angles suppress the $\chi_{MS}(k)_{am}$ signal coming from the atoms beyond the first shell. The subtraction of the double scattering contribution of the amorphous absorption spectrum in the r.h.s of eq. (4) can be important only for refining the agreement with the solid experimental curve in the wave vector range $k < 2\,\text{Å}^{-1}$. In the major part of the spectrum $[\chi_{MS}(k)]_{am}$ can be considered almost negligible, as it is also suggested by preliminary calculations of this signal. However this analysis cannot indicate the actual intensity of the MS contribution in the amorphous absorption spectrum because this very low signal can be hidden by the experimental noise.

4. Conclusions

This analysis has shown that the main features of the $[\alpha_{cr} - \alpha_{am}]/\alpha_0$ spectrum in the XANES energy region are due to multiple scattering effects.

The strong MS signal found in the crystalline absorption spectrum is almost suppressed in the amorphous one. The orientational disorder of bond angles is responsible of this quenching effect in the transition from the crystalline to the amorphous phase. In fact the amplitude of the MS signal depends on the existence of a large number of equal multiple scattering paths but in a disordered structure we have to consider an average value of the MS contribution over a broad distribution of MS path lengths. In this way the amplitude of the MS signal can provide a key for estimating the level of disorder of an amorphous system.

References

1. Bianconi, A., Incoccia, L. and Stipcich, S., EXAFS and near edge structure, edited by Springer series in Chem. Phys. **27**, (1983).
2. X-ray absorption: principle, applications, techniques of EXAFS, SEXAFS, XANES, (Edited by R. Prinz and D. Koningsberger), J. Wiley and sons, New York (1987).
3. Bianconi, A., Appl. Surf. Science **6**, 392 (1980).
4. Bianconi, A., Dell'Ariccia, M., Durham, P. J. and Pendry, J. B., Phys. Rev. **B26**, 6502 (1982).
5. Bianconi, A., Congiu-Castellano, A., Durham, P. J., Hasnain, S. S. and Philips, S., Nature **381**, 685 (1985).
6. Bianconi, A., Garcia, J., Marcelli, A., Benfatto, M., Natoli, C. R. and Davoli, I., Jour. de Physique **46**, C9-101 (1985).
7. Garcia, J., Benfatto, M., Natoli, C. R., Bianconi, A., Davoli, I. and Marcelli, A., Solid State Commun. **58**, 595 (1986).
8. Benfatto, M., Natoli, C. R., Bianconi, A., Garcia, J., Marcelli, A., Fanfoni, M. and Davoli, I., Phys. Rev. **B34**, 5774 (1986).
9. Durham, P. J., in Ref. [2] (1987).
10. Natoli, C. R. and Benfatto, M., Proc. of the international EXAFS and NES conference, Fontevraud (France), EXAFS and Near Edge Structure IV, Jour. de Physique, **47**, Colloque C8, 11 (1986).
11. Di Cicco, A., Pavel, N. V. and Bianconi, A., Solid State Commun. **61**, 635 (1987): Di Cicco, A., Bianconi, A., Pavel, N. V., Benfatto, M. and Natoli, C. R., Proc. of the international EXAFS and NES conference, Fontevraud (France), EXAFS and Near Edge Structure IV, Jour de Physique **47**, Colloque C8, 71 (1986).
12. Muller, J. E. and Schaich, W. L., Phys. Rev. **B27**, 6489 (1983).
13. Bunker, G. and Stern, E. A., Phys. Rev. Lett. **52**, 1990 (1984).
14. Lee, P. A. and Pendry, J. B., Phys. Rev. **B11**, 2795 (1975).
15. Bianconi, A., Di Cicco, A., Pavel, N. V., Benfatto, M., Marcelli, A., Natoli, C. R., Pianetta, P. and Woicik, J., Phys. Rev. B **36**, 6426 (1987).
16. Lengeler, B. and Eisenberger, P., Phys. Rev. **B21**, 4507 (1980).
17. Muller, J. E., Jepsen, O. and Wilkins, J. W., Solid State Commun. **42**, 365 (1982).
18. Sevillano, E., Meuth, H. and Rehr, J. J., Phys. Rev. **B20**, 4908 (1979).
19. Walker, C. B. and Keating, D. T., Acta Cryst. **14**, 1170 (1961).
20. Evangelisti, F., Proietti, M. G., Balzarotti, A., Comin, F., Incoccia, L. and Mobilio, S., Solid State Commun. **37**, 413 (1981).
21. Balerna, A., Benfatto, M., Molilio, S., Natoli, C. R., Filipponi, A. and Evangelisti, F., Proc. of the international EXAFS and NES conference, Fontevraud (France), EXAFS and Near Edge Structure IV, Journal de Physique, **47**, Colloque C8, 63 (1986).
22. Connell, G. A. N. and Temkin, R. J., Phys. Rev. **B9**, 5323 (1974).
23. Wooten, F., Winer, K. and Weaire, D., Phys. Rev. Lett. **54**, 1392 (1985).